Electronic Supplementary Material (ESI) for Journal of Materials Chemistry A.

Electronic Supplementary Information

Crystal Phase Tuning and Valence Engineering in Non-noble Catalyst for Outstanding Overall Water Splitting

Kailing Zhou,[a] Qianqian Zhang,[a] Jingbing Liu, [a] Hao Wang*[a] and Yongzhe Zhang[a]

[a] College of Materials Science and Engineering, Beijing University of Technology, Beijing 100124, P. R. China. E-mail: haowang@bjut.edu.cn

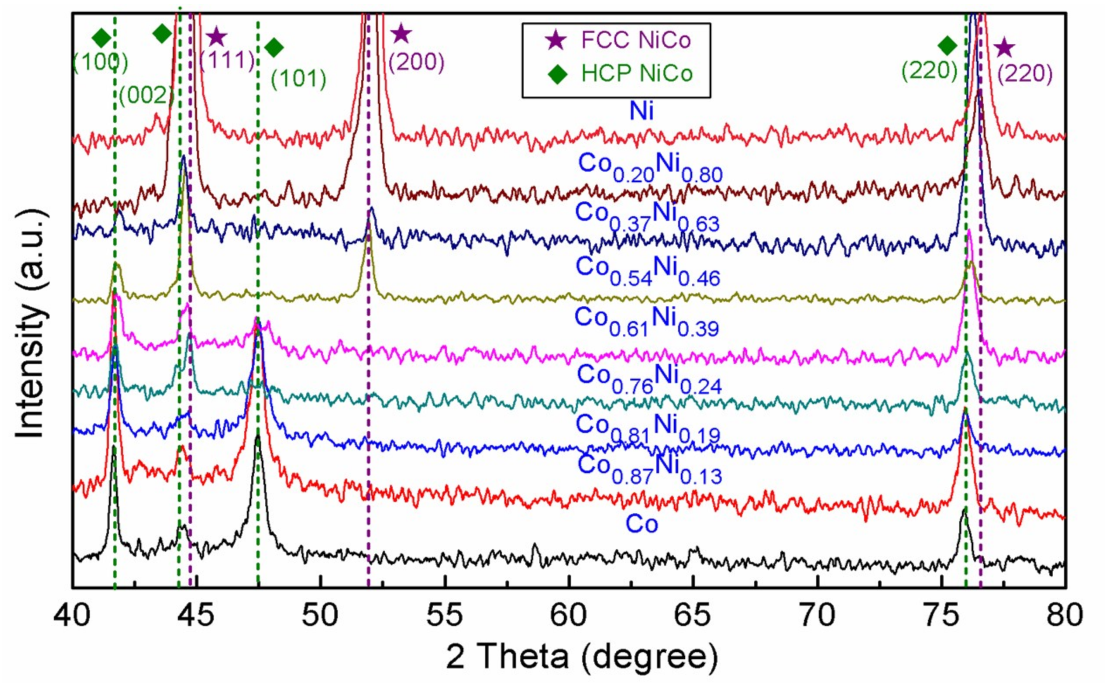

Figure S1. XRD patterns of as-synthesized Ni_xCo_{1-x} alloys with the different Ni contents.

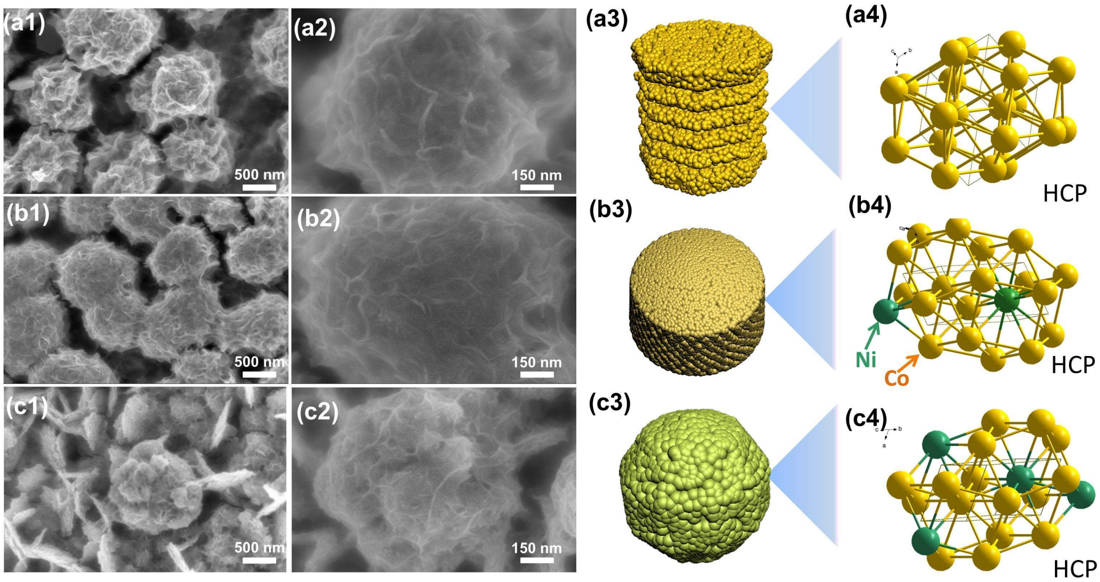

Figure S2. The SEM image of samples (a1-2) Co, (b1-2) $Ni_{0.13}Co_{0.87}$ and (c1-2) $Ni_{0.19}Co_{0.81}$, corresponding nanostructural model and the simple schematic diagram of crystal phase (a3-4, b3-4, c3-4).

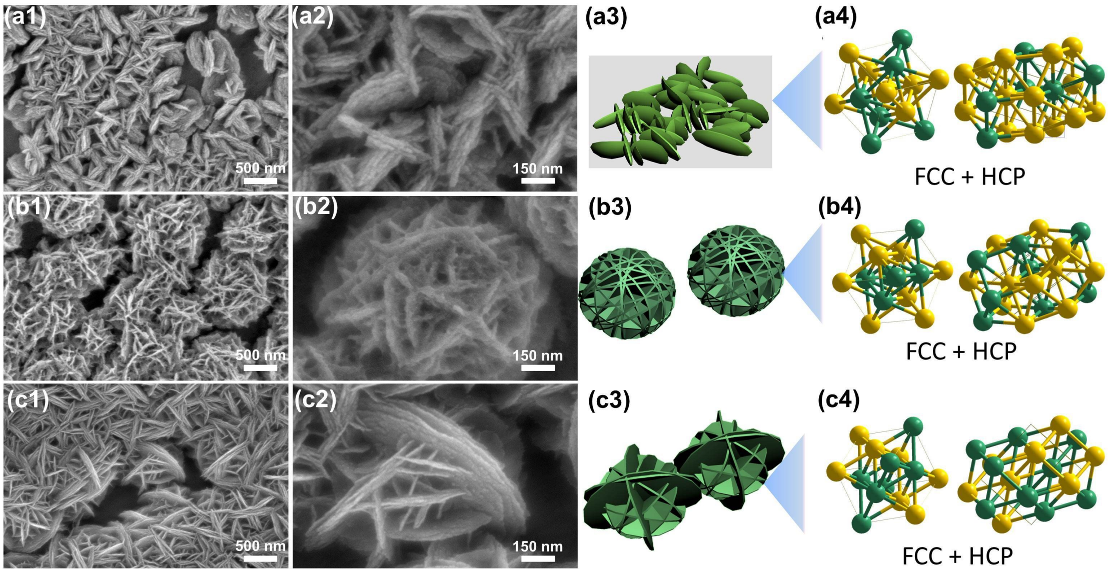

Figure S3. The SEM image of samples (a1-2) $Ni_{0.24}Co_{0.76}$, (b1-2) $Ni_{0.39}Co_{0.61}$ and (c1-2) $Ni_{0.46}Co_{0.54}$, corresponding nanostructural model and the simple schematic diagram of crystal phase (a3-4, b3-4, c3-4).

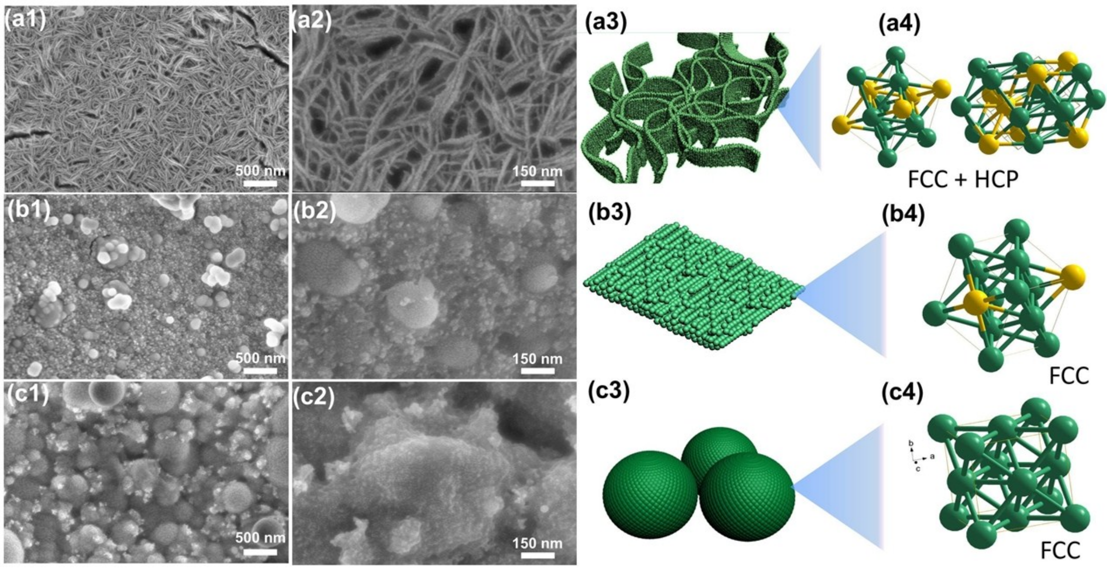

Figure S4. The SEM image of samples (a1-2) $Ni_{0.63}Co_{0.37}$, (b1-2) $Ni_{0.80}Co_{0.20}$ and (c1-2) Ni, corresponding nanostructural model and the simple schematic diagram of crystal phase (a3-4, b3-4, c3-4).

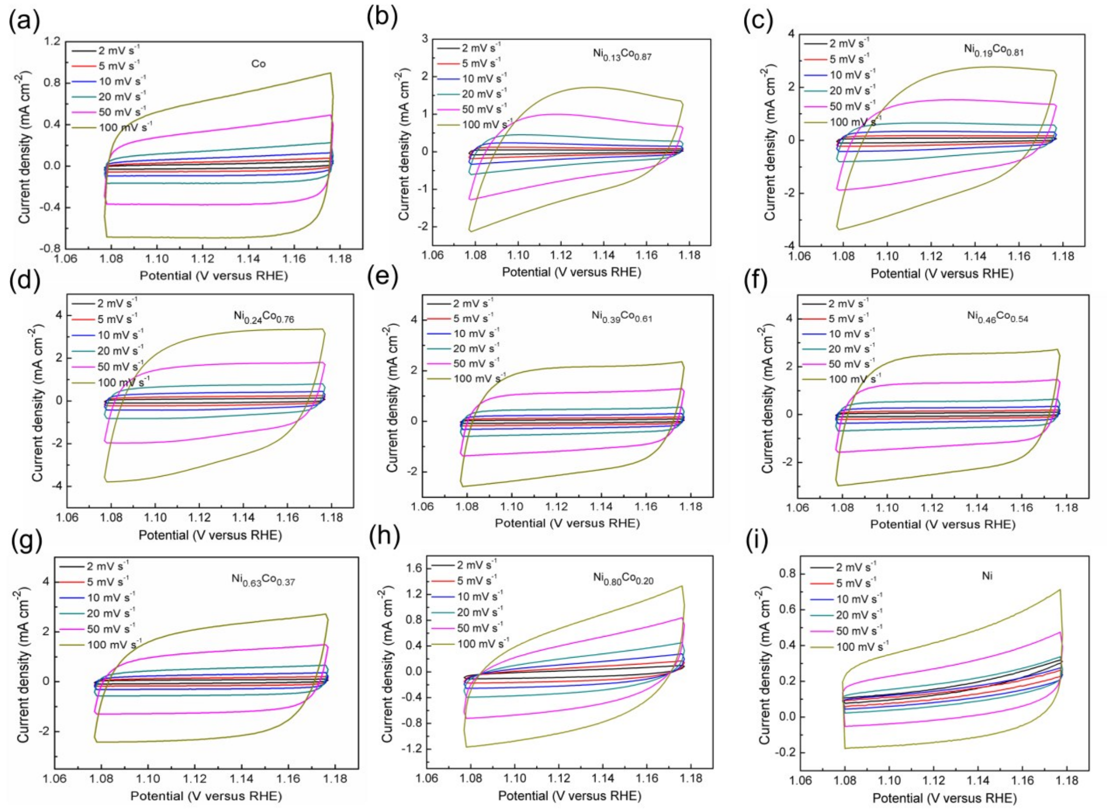

Figure S5. Cyclic voltammograms obtained with Co, $Ni_{0.13}Co_{0.87}$, $Ni_{0.19}Co_{0.81}$, $Ni_{0.24}Co_{0.76}$, $Ni_{0.39}Co_{0.61}$, $Ni_{0.46}Co_{0.54}$, $Ni_{0.63}Co_{0.37}$, $Ni_{0.80}Co_{0.20}$ and Ni alloy electrodes, respectively.

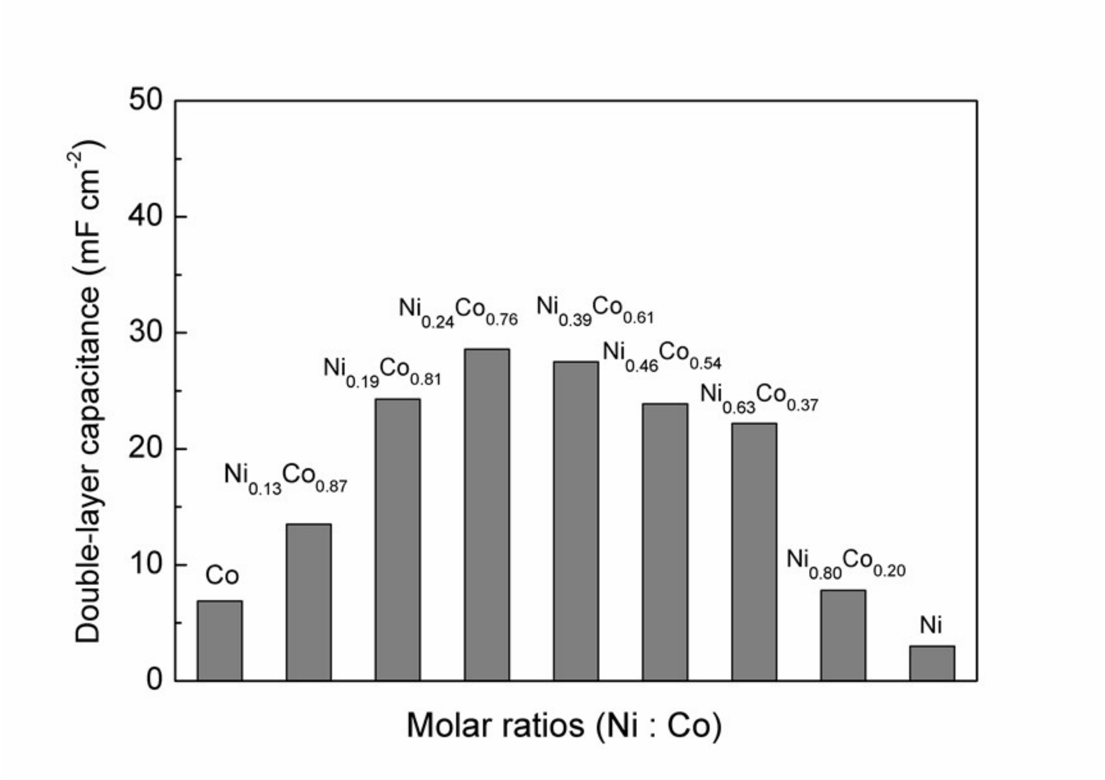

Figure S6. The Double-layer capacitance (C_{dl}) plotted as a function of molar ratio between Ni and Co in alloy electrodes.

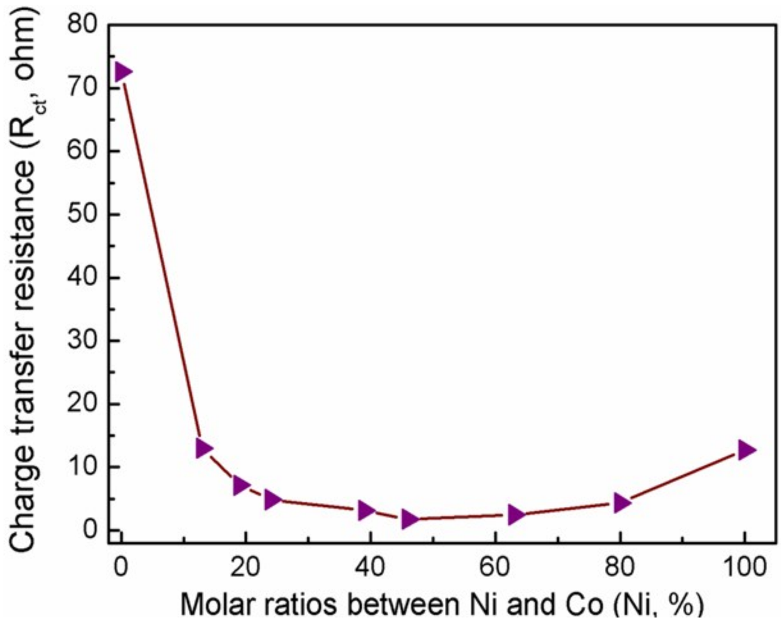

Figure S7. The charge transfer resistance (R_{ct}) plotted as a function of the molar ratio between Ni and Co in alloy electrodes.

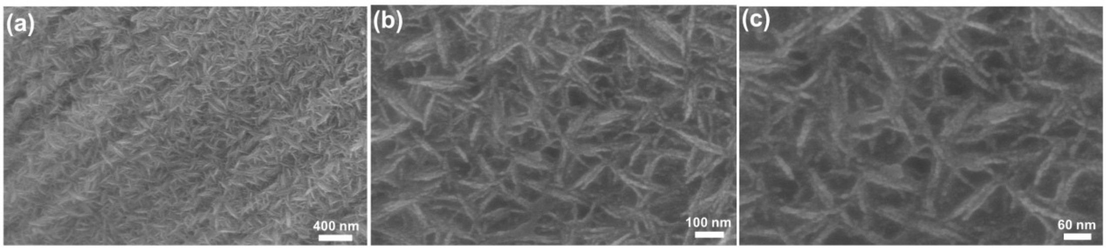

Figure S8. The SEM image of $Ni_{0.46}Co_{0.54}$ alloy electrode at the initial stage of electrochemical growth.

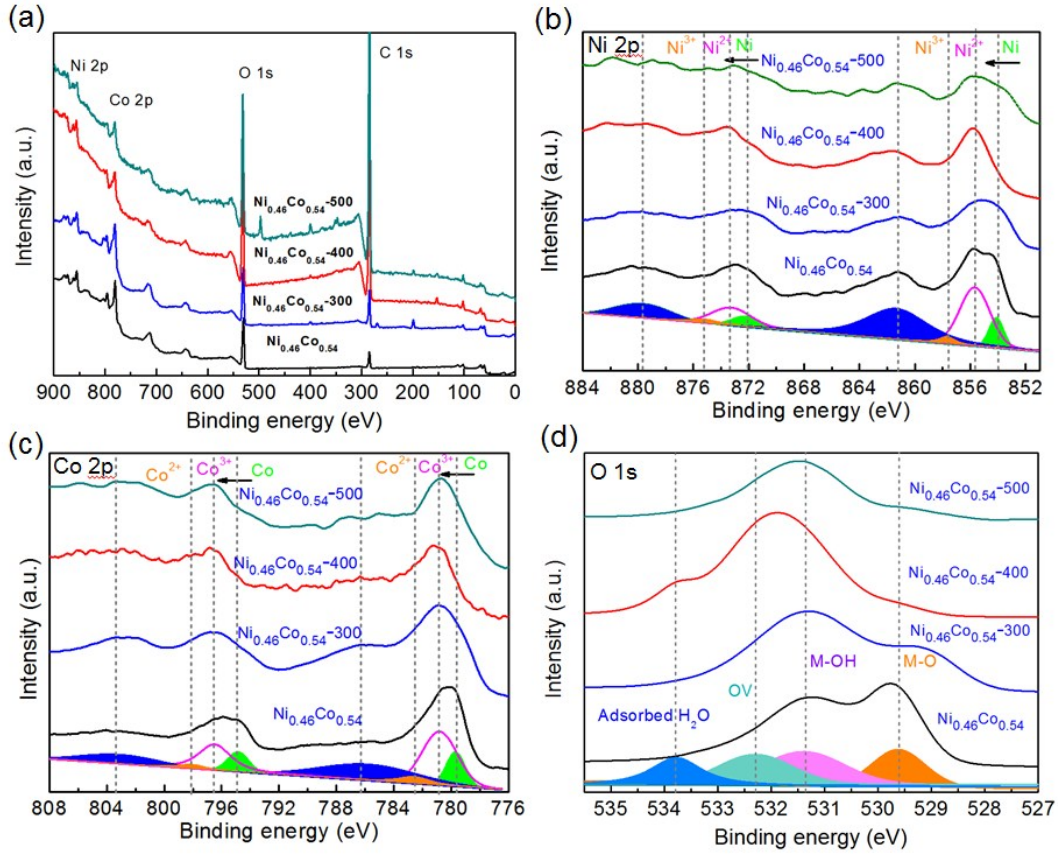

Figure S9. (a) The XPS survey spectra and the high-resolution Ni 2p (b), Co 2p (c) and O 1s (d) XPS spectra of $Ni_{0.46}Co_{0.54}$, $Ni_{0.46}Co_{0.54}$-300, $Ni_{0.46}Co_{0.54}$-400 and $Ni_{0.46}Co_{0.54}$-500.

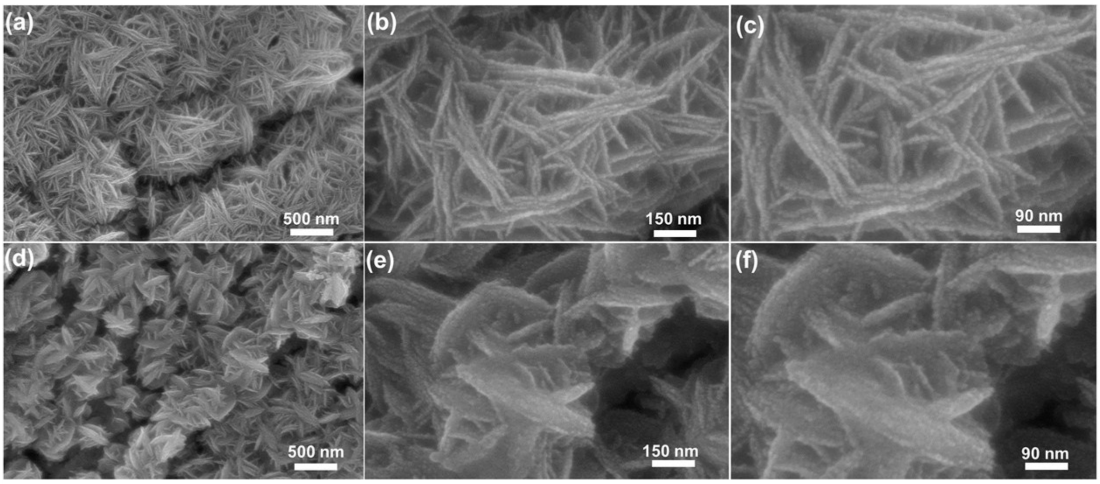

Figure S10. The SEM images with different magnifications of $Ni_{0.46}Co_{0.54}$ alloy after (a-c) 300 °C and (d-f) 500 °C annealing treatment in an air atmosphere.

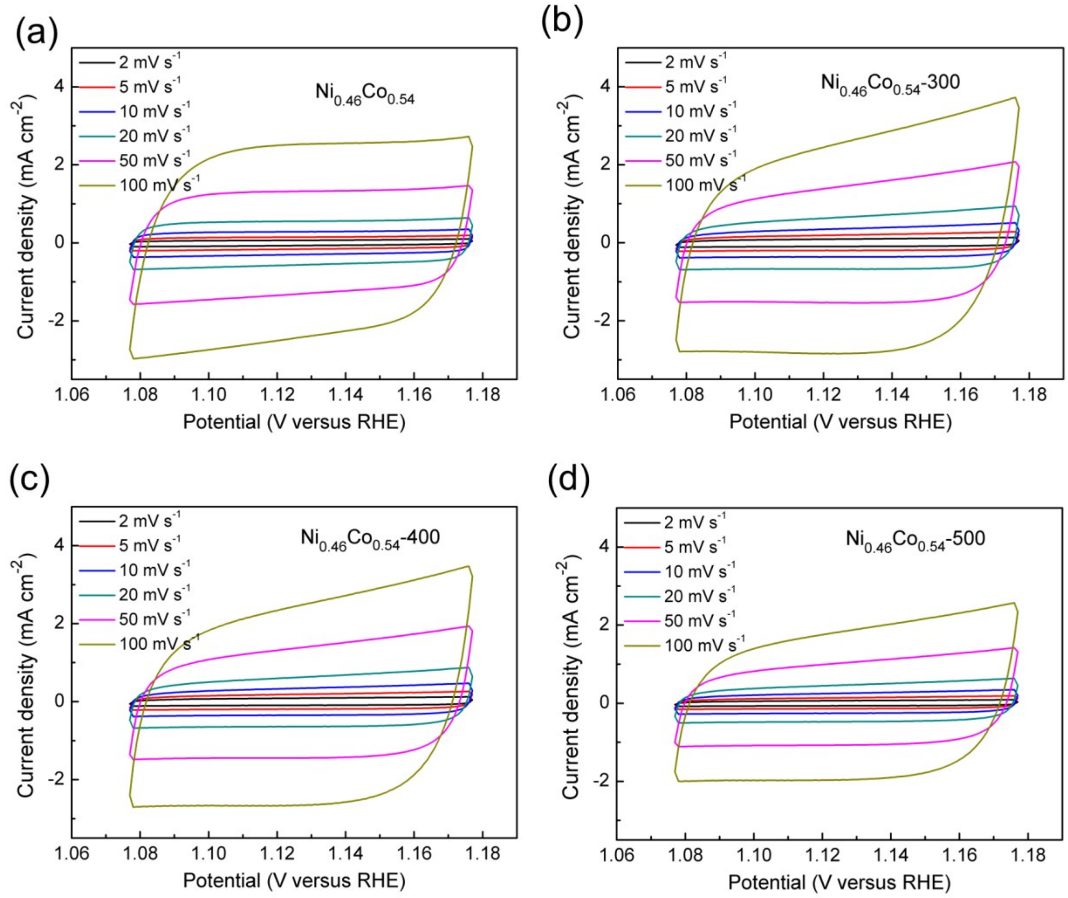

Figure S11. Cyclic voltammograms obtained with (a) $Ni_{0.46}Co_{0.54}$, (b) $Ni_{0.46}Co_{0.54}$-300, (c) $Ni_{0.46}Co_{0.54}$-400 and (d) $Ni_{0.46}Co_{0.54}$-500 in the capacitance potential range (-1.08 V ~ 1.18 V versus RHE) at scan rates of 2, 5, 10, 20, 50 and 100, respectively.

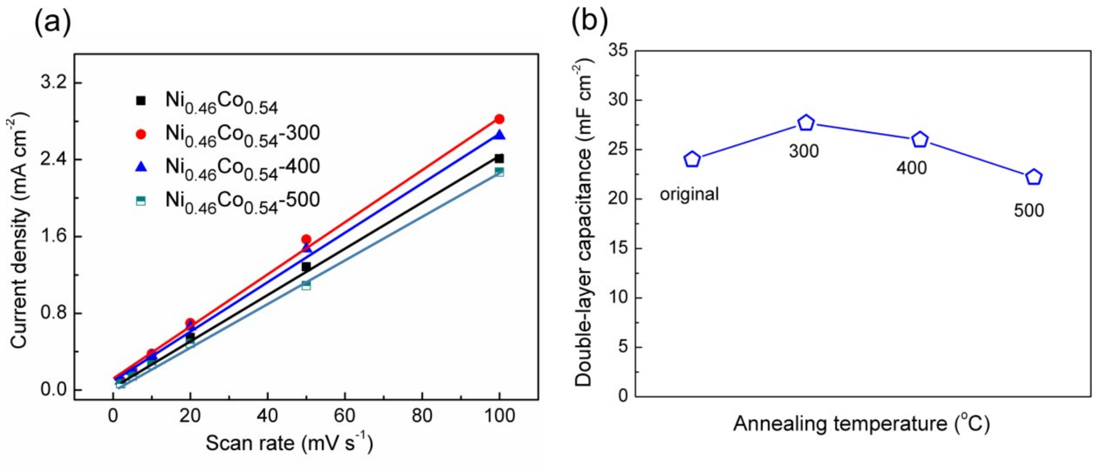

Figure S12. (a) Charging current density differences plotted against scan rate for $Ni_{0.46}Co_{0.54}$-based electrode. The linear slope is equivalent to the double-layer capacitance C_{dl}, representing the electrochemical surface area. (b) The double-layer capacitance C_{dl} plotted against annealing temperature.

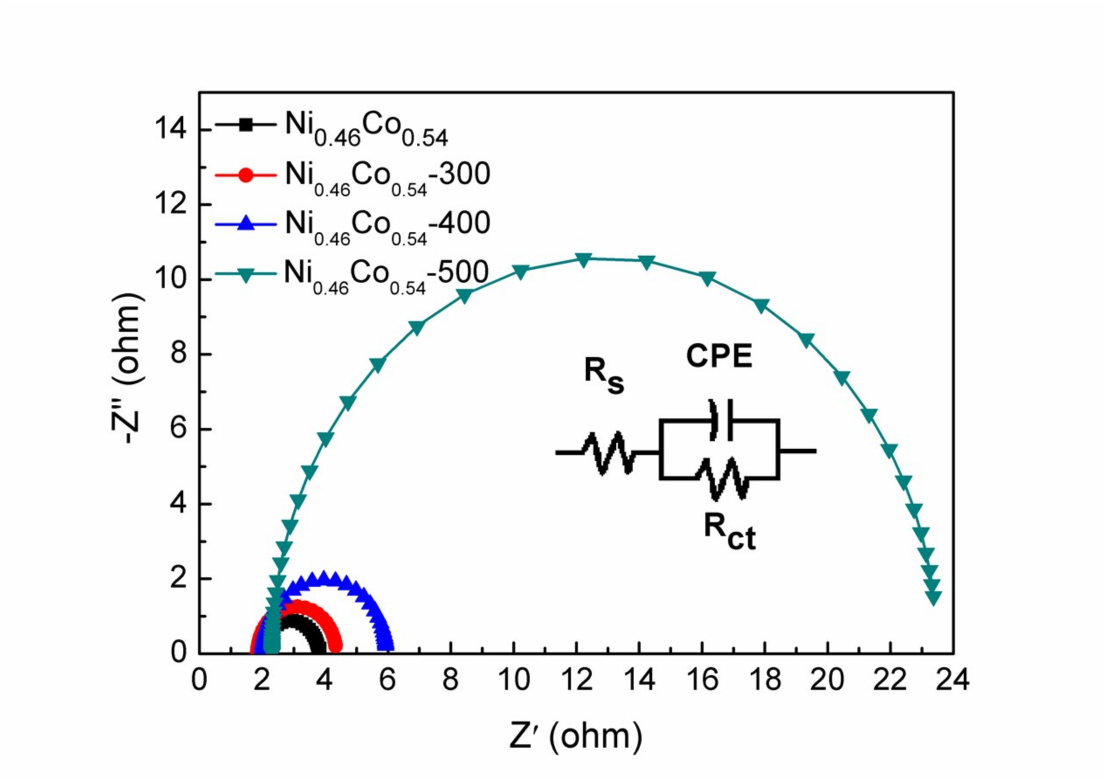

Figure S13. Nyquist plots of $Ni_{0.46}Co_{0.54}$-based electrode for HER measured at -183 mV vs RHE.

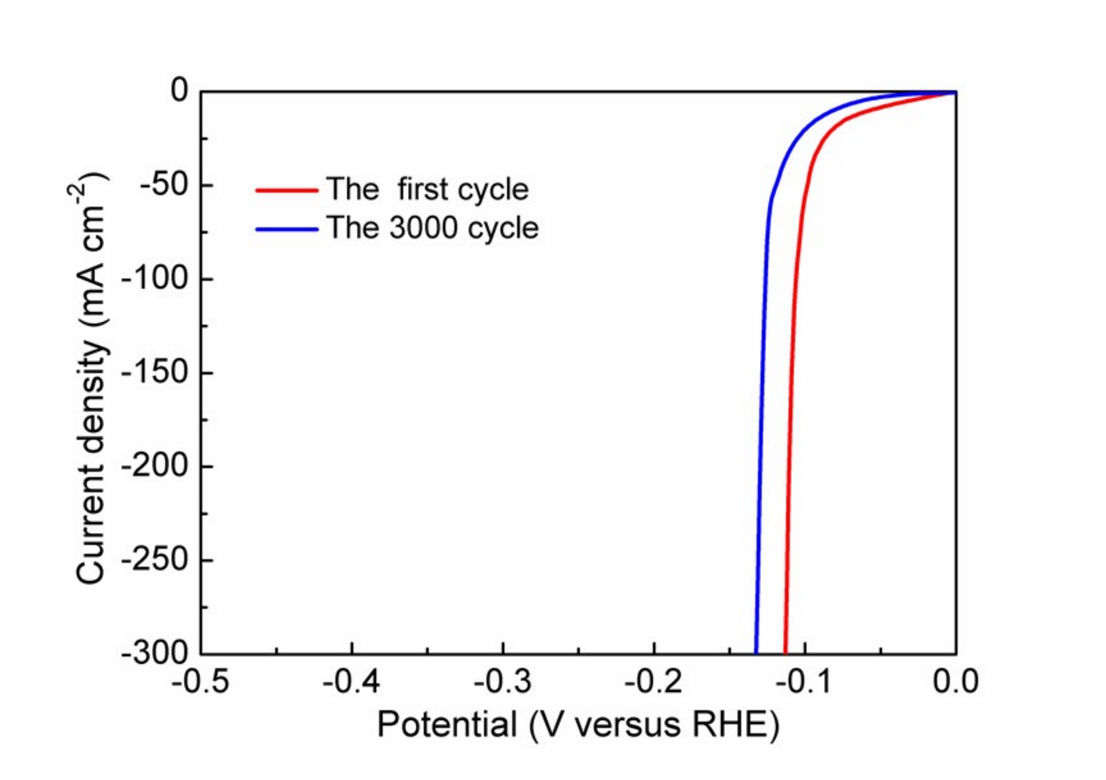

Figure S14. Cyclic voltammetry (CV) curves of $Ni_{0.46}Co_{0.54}$-400 electrode before and after the HER durability test with 3000 cycles.

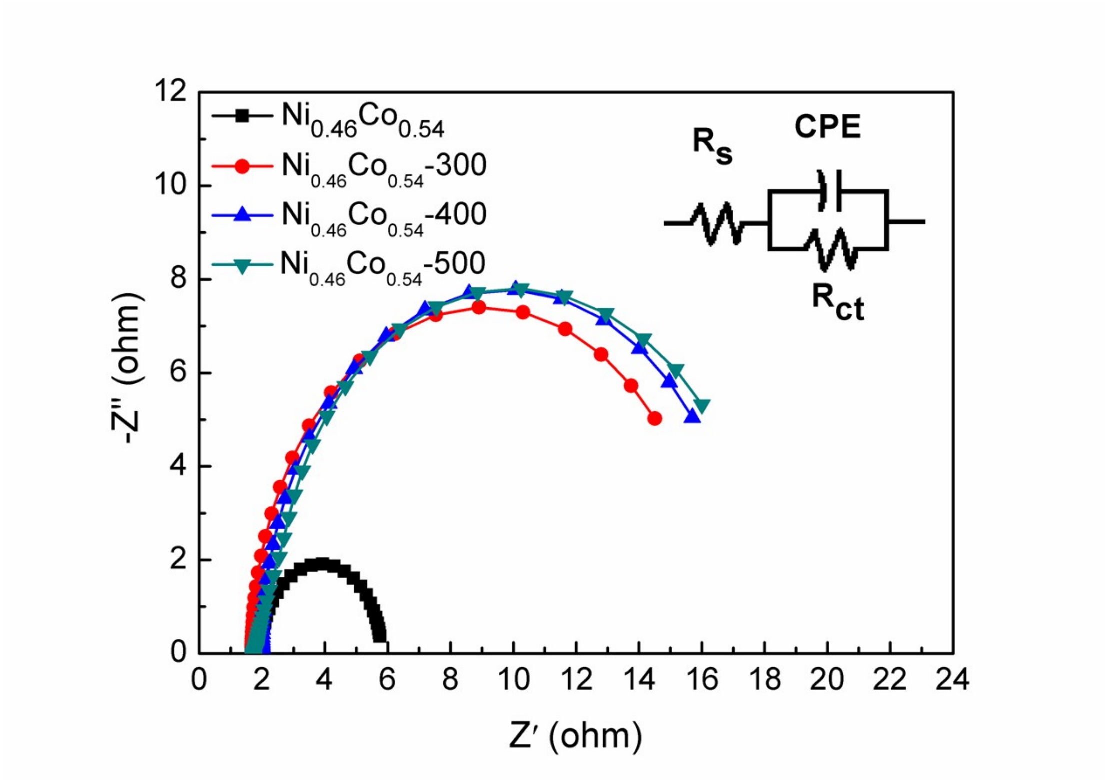

Figure S15. Nyquist plots of $Ni_{0.46}Co_{0.54}$-based electrodes measured at 1.517 V vs RHE for OER.

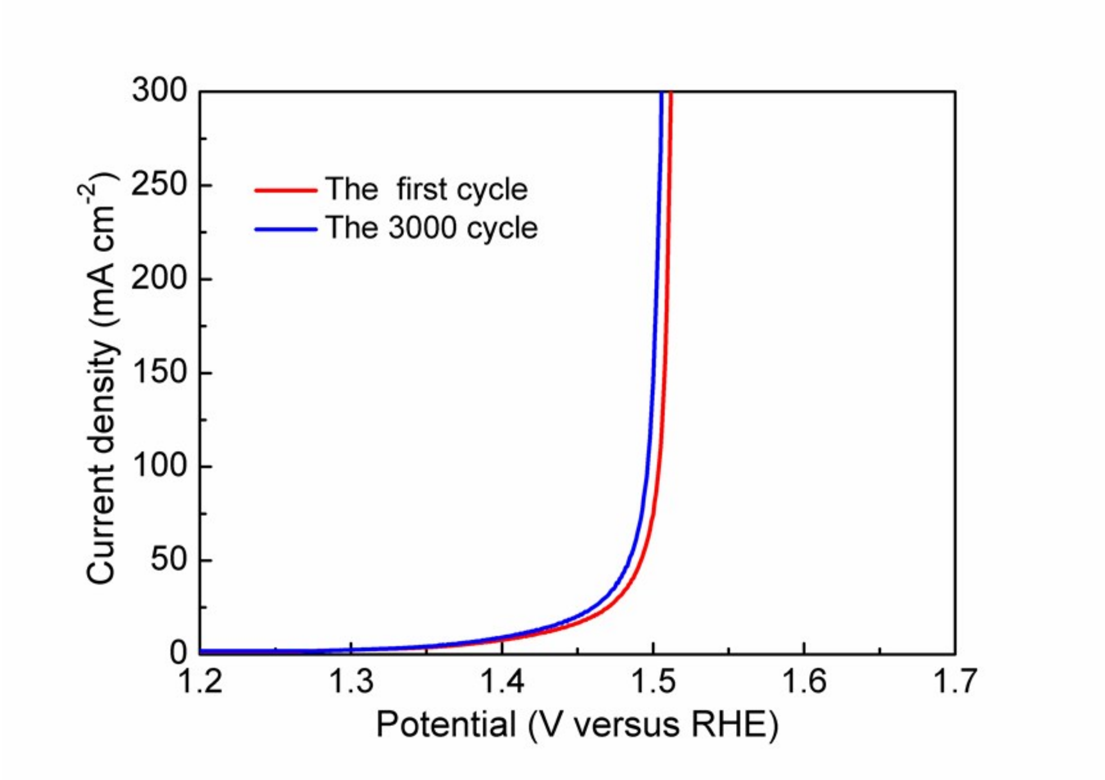

Figure S16. Cyclic voltammetry (CV) curves of $Ni_{0.46}Co_{0.54}$-400 electrode before and after the OER durability test with 3000 cycles.

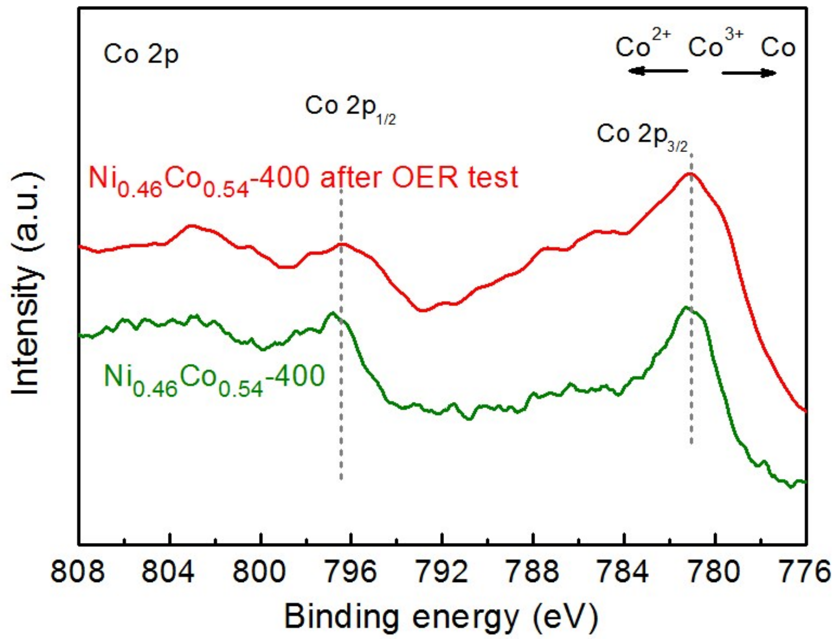

Figure S17. XPS spectra evolution of Co 2p in initial $CoNiO_2/Ni_{0.46}Co_{0.54}$ and after OER electrocatalysis with 3000 cycles. No apparent change can be found, suggesting the stable nature of $CoNiO_2/Ni_{0.46}Co_{0.54}$ for OER.

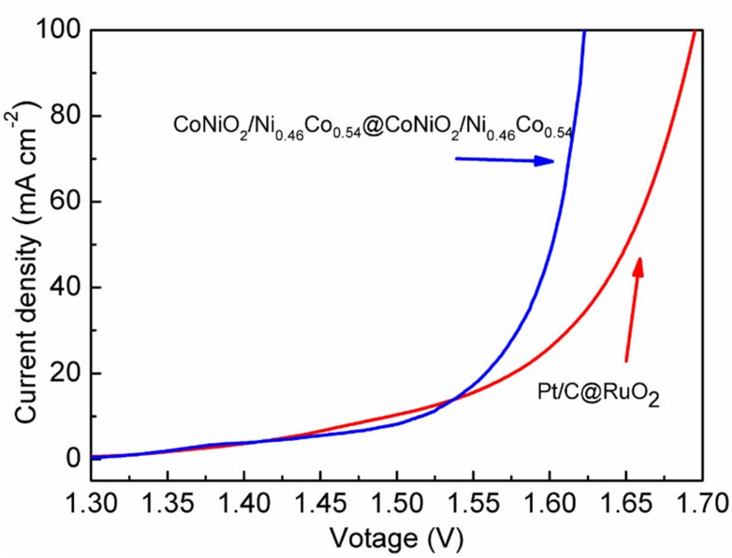

Figure S18. The performance of $Pt/C@RuO_2$ for overall water splitting

Table S1. Comparison of HER performances of $Ni_{0.46}Co_{0.54}$-400 catalyst with recently reported catalysts in alkaline electrolyte.

Electrocatalysts	Overpotential at 10 mA cm^{-2} (mV)	Tafel slop (mV dec^{-1})	Loading mass	Reference
$Ni_{0.46}Co_{0.54}$-400	58	36	0.46 mg cm^{-2}	This work
$NiCo_2S_4$ nanowire	210	58.9	-	*Adv. Funct. Mater*. **2016**, 26, 4661.
$Ni_{0.33}Co_{0.67}Se_2$	106	60	-	*Adv. Energy Mater.* **2017**, 7, 1602089.
CoMoP@C	81	55	0.35 mg cm^{-2}	*Energy Environ. Sci.,* **2017**, 10, 788.
NiO/Ni-CNT	80	51	8.00 mg cm^{-2}	*Nat. Commun.* **2014**, 5, 4695.
N-$NiCo_2S_4$ nanowire	41	37	-	*Nat. Commun.* 2018, 9(1): 1425.
$Pt_{13}Cu_{73}Ni_{14}$	148	54	-	*ACS Appl. Mater. Interfaces* **2016**, 8, 3464.
MoO_x/Ni_3S_2/NF	106	90	12.00 mg cm^{-2}	Adv. Funct. Mater. **2016**, 26, 4839.
NF–Ni_3Se_2/Ni	203	79	8.87 mg cm^{-2}	Nano Energy **2016**, 24, 103.
Mn-CoP/Ti	76	52	5.61 mg cm^{-2}	*ACS Catal.* **2016**, 7, 98.
CoS_2	98	57	0.34 mg cm^{-2}	*ACS Energy Lett.* **2018**, 3, 779.
N,Mn-MoS_2/NF	66	50	4.00 mg cm^{-2}	*ACS Catal.* **2018**, 8, 7585.
$Ni_{0.89}Co_{0.11}Se_2$	85	52	2.62 mg cm^{-2}	*Adv. Mater.* **2017**, 29, 1606521
$NiCo_2P_x$/CC	58	34	5.90 mg cm^{-2}	*Adv. Mater.* **2017**, 29, 1605502.
Ce-doped CoP/Ti	92	64	-	*Nano Energy* **2017**, 38, 290.

Table S2. Comparison of OER performances of $Ni_{0.46}Co_{0.54}$-400 catalyst with recently reported catalysts in alkaline electrolyte.

Electrocatalysts	Overpotential at 10 mA cm^{-2} (mV)	Tafel slop (mV dec^{-1})	Loading mass	Reference
$Ni_{0.46}Co_{0.54}$-400	195	30	0.46 mg cm^{-2}	This work
NiFe LDH	244	32	-	*Nat. Commun.* **2016,** 7, 12324.
Gelled FeCoW	191	37	0.21 mg cm^{-2}	*Science* **2016**, 352, 333.
EG/$Co_{0.85}$Se/NiFe LDH	203	57	4.00 mg cm^{-2}	Energy Environ. Sci. **2016**, 9, 478
$NiCeO_x$–Au	270	-	-	*Nat. Energy* **2016**, 1, 16053.
$NiCo_2O_4$	290	-	1.00 mg cm^{-2}	*Angew. Chem. Int. Ed.* **2016**,55, 6290
CoFePO	275	52	2.18 mg cm^{-2}	*ACS Nano* **2016**, 10, 8738
NiFe-LDH/ $NiCo_2O_4$ /NF	290	53	4.90 mg cm^{-2}	*ACS Appl. Mater. Interfaces,* **2017**, 9, 1488
Co-MoS_2	260	85	2.00 mg cm^{-2}	*Adv. Mater.* **2018**, 1801450
FeCoNi-LTH	302	72	-	*ACS Appl. Mater. Interfaces* **2017**, 9, 36917
$Ni_{1.5}Fe_{0.5}$P/CF	264	55	1.38 mg cm^{-2}	*Nano Energy* **2017**, 34, 472
Ni_3FeN-NPs	280	46	0.20 mg cm^{-2}	*Adv. Energy Mater.* **2016**, 6, 1502585
NiCoFe@NiCoFeO NTAs/CFC	201	39	-	*J. Am. Chem. Soc.* **2019**, 20, 8136.
NiCo/pNGr	260	87	1.00 mg cm^{-2}	*Adv. Mater. Interfaces* **2016**, 3, 1600532.
CoFe LDHs	300	83	0.20 mg cm^{-2}	*ChemPlusChem* **2017**, 82, 483.

Table S3. Comparison of overall water splitting performances of $Ni_{0.46}Co_{0.54}$-400 catalyst with recently reported catalysts in alkaline electrolyte.

Electrocatalysts	Cell voltage at 10 mA cm^{-2} (V)	1.65 V mA	Loading mass	Reference
$Ni_{0.46}Co_{0.54}$-400	1.51	234	0.46 mg cm^{-2}	This work
hierarchical Ni-Co-P HNBs	1.62	20	2.00 mg cm^{-2}	*Energy Environ. Sci.* **2018**, 11, 872.
$NiFeO_x$	1.51	48	1.60 mg cm^{-2}	*Nat. Commun.* **2015**, 6, 7261
Co−Mn carbonate hydroxide	1.68	12	5.60 mg cm^{-2}	*J. Am. Chem. Soc.* **2017**, 139, 8320.
Cu@CoFe LDH	1.62	15	1.80 mg cm^{-2}	*Nano Energy* **2017**, 41, 327.
MoS_2/NiS_2 nanosheets	1.59	27	1.10 mg cm^{-2}	*Adv. Sci.* **2019**, 6, 1900246.
FeCoNi-1T' MoS_2	1.42	68	-	*Nat. Commun.* **2018**, 9, 2452.
CoFeZr oxides /NF	1.63	18	-	*Adv. Mater.* **2019**, 31, 1901439
$Ni_{0.51}Fe_{0.49}P$ film	1.57	85	-	*Adv. Funct. Mater.* **2016**, 26, 7644.
NiFe LDH/Cu NW	1.54	67	-	*Energy Environ. Sci.* 2017, 10, 1820.
FeP/Ni_2P	1.42	210	8.00 mg cm^{-2}	Nat. Commun. **2018**, 9, 2551.
MoS_2/Ni_3S_2	1.56	80	9.70 mg cm^{-2}	*Angew. Chem. Int. Ed.* **2016**, 55, 6702.
MoS_2/NiFe-LDH	1.57	42	0.21 mg cm^{-2}	*Nano Lett.* **2019**, 19, 4518.
Ni_3N-VN/NF/Ni_2P-VP_2/NF	1.51	30	-	*Adv. Mater.* **2019**, 31, 1901174
Ni QD@NC@rGO	1.56	38	1.00 mg cm^{-2}	*Appl. Catal. B: Environ.* **2019**, 250, 213.
$Co(OH)_2$@NCNTs@NF	1.72	-	0.72 mg cm^{-2}	*Nano Energy* **2018**, 47, 96
CoP/GO-400	1.70	-	0.28 mg cm^{-2}	*Chem. Sci.* **2016**, 7, 1690

NiS/Ni foam	1.64	-	0.28 mg cm^{-2}	*ACS Catal.* **2018**, 8, 2236
NiCo-LDH/NF	1.66	-	1.00 mg cm^{-2}	*Dalton Trans*. **2017**, 46, 8372